RSC Advances

ROYAL SOCIETY OF CHEMISTRY

www.rsc.org/advances

Journal Name

ARTICLE

Non-corrosive α-alumina@TiO_2 core-shell nanoplates appearing metallic gold in colour

Received 00th January 20xx,
Accepted 00th January 20xx

DOI: 10.1039/x0xx00000x

www.rsc.org/

Myung Won Suh,[a,†] Su Jin Lee,[b,†] Myoung Sang You,[b] Seung Bin Park[a,*] and Sang Hyuk Im[b,*]

Non-corrosive α-alumina@TiO_2 core-shell nanoplates exhibiting lustring metallic gold in colour were synthesized by sol-gel solution chemistry with controlled reaction condition for the formation of anatase and rutile TiO_2 nanocrystals. Due to the small mismatch of lattice parameter between rutile TiO_2 and two-dimensional α-alumina nanoplates, the rutile TiO_2 could be conformably grown on the surface of α-alumina nanoplates, however, the lustring effect was deteriorated by the back scattering due to the formation of rough needle-shaped rutile TiO_2. The surface roughness of TiO_2 nano-shell was controlled by pH control of the reactant solution because rutile phase TiO_2 nanocrystals tend to be formed in more acidic condition, whereas anatase pahse TiO_2 is likely to be promoted in less acidic condition, of which anatase small nanocrystals smothen the surface of TiO_2 nano-shell during the crystal growth. The successful formation of smooth TiO_2 nano-shell via controlled crystal growth was associated with the fact that the intermedate complex of $[Ti(OH)_mCl_n]^{2-}$ (m+n=6) tends to make edge sharing in more acidic condition and coner sharing in less acidic condition. Apparently the α-alumina@TiO_2 core-shell nanoplates prepared in more and less acidic condition showed metallic gold in colour, however, the core-shell nanoplates synthesized in less acidic condition exhibted better lustring effect than those in more acidic condition due to the formation of smooth TiO_2 shell.

Introduction

Two-dimensional (2D) nanoplates such as graphene, metals, semi-conductors, and metal oxides have been of great interest because of their potential in applications to flexible transparent electrode,[1] barrier film,[2] thin film transistor,[3] stretchable electrode,[4] and colour pigment[5]. Among them, the metal oxide 2D nanoplates including glass,[6] mica,[7] and alumina nanoflake[8] have been extensively utilized in pigment industry because they can show lustring colour and the colour can be controlled by coating thickness and refractive index of shell material. Hence, the lustring colour is originated by the constructive and deconstructive interference of light at air/shell/2D metal oxide nanoplate interface, thereby exhibiting angle dependent structure colouring like one-dimensional photonic crystals. For instance, if we assume that the incident light with θ angle from the normal direction is reflected at shell(n_s)/2D metal oxide nanoplate (n_m) interface, the constructive interference is occurred when it satisfies following condition:[9]

$$2n_s d\cos\theta = m\lambda \qquad (1)$$

Where, n_s is refractive index of shell, n_m is refractive index of shell, d is thickness of shell, m is integer, and λ is wavelength, respectively. The reflectance (R) can be written by following equation:[9]

$$R = \frac{n_s^2(n_a - n_m)^2\cos^2\delta + (n_a n_m - n_s^2)^2\sin^2\delta}{n_s^2(n_a + n_m)^2\cos^2\delta + (n_a n_m + n_s^2)^2\sin^2\delta} \qquad (2)$$

Where, n_a is refractive index of air and δ is $2\pi n_s d\cos\theta/\lambda$, respectively. Therefore, the colour of reflected light is dependent on the thickness (d), refractive index (n_s), and incident angle (θ) of shell. Moreover, the intensity of reflected light is closely related to refractive index of each layer and refractive index difference between each layer. In particular, here the n_a and n_m is fixed to air (n_a = 1.0) and α-alumina (n_m = 1.7) so that the n_s is important to maximize lustring effect. Namely, higher refractive index materials such as crystalline TiO_2 are more desirable for shell material to show better lustring effect.

Initially, the pearlescent 2D pigments were obtained from the fish scales of hair tails or herrings because the synthetic technology for the artificial 2D pigments was not developed. Although the crystalline 2D guanine or hypoxanthine natural pigments can be collected from the fish scales, the yield was very low to cope with the demands for pearlescent pigments.

---

[a] *Department of Chemical and Biomolecular Engineering, Korea Advanced Institute of Science and Technology (KAIST), 291 Daehak-ro, Yuseong-gu, Daejeon 305-701, Republic of Korea. E-mail:sbpark7@kaist.ac.kr*

[b] *Functional Crystallization Center (FCC), Department of Chemical Engineering, Kyung Hee University, 1732 Deogyeong-daero, Giheung-gu, Yongin-si, Gyeonggi-do 446-701, Republic of Korea. E-mail:imromy@khu.ac.kr*

† M. Y. Suh and S. J. Lee contributed equally to this work.

Electronic Supplementary Information (ESI) available: [details of any supplementary information available should be included here]. See DOI: 10.1039/x0xx00000x

Therefore, the artificial 2D pearlescent pigments such as basic lead carbonate ($Pb(OH)_2 \cdot 2PbCO_3$), bismuth oxychloride (BiOCl), glass, and mica have been synthesized.[5] Among them, the 2D mica pigments have been widely used until now because the natural mica could be easily collected from mine. However, the natural mica often reveals non-uniform colour or yellowish in colour because the composition of impurities in natural mica differs from the location of mine. Mica is composed by complex hydrous potassium-aluminium silicate and consequently has various names such as biotite, lepidolite, muscovite, phlogopite, and vermiculite according to its chemical composition.[7a] Therefore, mica exhibits different colour according to the variation of its chemical composition. In addition, the mica requires additives to coat TiO_2 on its surface and the control of surface roughness of TiO_2 shell is difficult, as well.[7c,d] Accordingly, 2D α-alumina nanoplates will be better as a mother substrate than the mica because α-alumina has pure phase and small lattice mismatch with rutile TiO_2. Here, we tried to coat TiO_2 nano-shell on the surface of α-alumina nanoplates in order to synthesize non-corrosive pigments with metallic gold in colour because TiO_2 is very stable metal oxide which is not corroded by most acid or base chemicals.

Experimental

Materials

2D α-alumina nanoplate was purchased from TCERA. $TiCl_4$ (Titanium tetrachloride), HCl, and NaOH was purchased from Fluka, Samchun, and Samchun, respectively. We used the chemicals as it received without further purification.

Characterization

For the analysis of scanning electron microscopic (SEM: Supra 55, Carl Zeiss) image of samples, we dropped 2D α-alumina nanoplate or 2D α-alumina@TiO_2 core-shell nanoplates or TiO_2 nanoparticles dispersion solution on a Si wafer and dried them. The dried samples were then coated by Pt by sputter. For the analysis of transmission electron microscopic (TEM: Jem-2100F, Jeol) image, we dropped the TiO_2 nano-sol solution on a carbon coated Cu grid. For the analysis of X-ray diffraction (XRD: D8 advance, Bruker) patterns, we collected the dried powder of 2D α-alumina nanoplate or 2D α-alumina@TiO_2 core-shell nanoplates or TiO_2 nanoparticles and placed them on Si low background sample holder. The scanned the samples from 20^o to 80^o at a scan rate of 6^o/min under irradiation of Cu K-α (λ=0.15406 nm).

Results and discussion

A scanning electron microscopic (SEM) image of 2D α-alumina nanoplate in Fig. 1(a) indicates that the lateral size and thickness of nanoplate is 10-30 μm and ~500 nm, respectively. Fig. 1(b) is magnified SEM image of a white rectangle in Fig. 1(a) indicating that the surface of the nanoplate is uniform. This indicates that the 2D nanoplates are adaptable to the substrates for interference pearlescent pigments. Fig. 1(c) is a photograph of 2D α-alumina nanoplates which are prepared by dropping a 2D α-alumina nanoplates/water dispersion solution on a glass plate and subsequent drying. The pristine 2D α-alumina nanoplates exhibited metallic silver in colour. Fig. 1(d) is X-ray diffraction (XRD) patterns of 2D nanoplates indicating that the nanoplates have crystalline α-alumina phase.

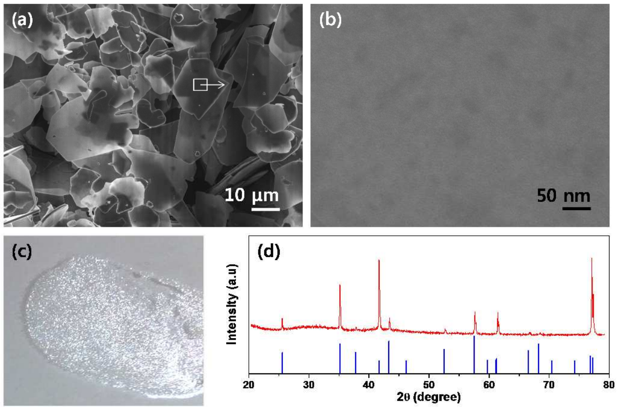

Fig. 1. (a) A scanning electron microscopic (SEM) image of 2D α-alumina nanoplates (TCERA), (b) magnified SEM image of white rectangle part in Fig. 1(a), (c) photograph of 2D α-alumina nanoplates, and (d) X-ray diffraction (XRD) patterns: red peak = sample, blue line = JCPDS# 82-1468 .

Table 1 summarized the material properties of crystalline α-Al_2O_3, rutile TiO_2, and anatase TiO_2 indicating that the lattice parameter of rutile TiO_2 is slightly mismatched with the lattice parameter of α-Al_2O_3, wherease the anatase TiO_2 has great lattice mismatch with the α-Al_2O_3. In addition, the refractive index of rutile TiO_2 is higher than the anatase TiO_2 so that the lustring effect is more enhanced by the rutile TiO_2. Therefore, here, we tried to coat rutile TiO_2 nano-shell on the surface of 2D α-alumina nanoplates in order to make pearlescent metallic gold in colour.

Table 1. Summary of material properties of crystalline α -Al_2O_3, rutile TiO_2, and anatase TiO_2.

Properties	α -Al_2O_3	Rutile	Anatase
Crystal system	Hexagonal	Tetragonal	Tetragonal
a	4.75 Å	4.59 Å	3.78 Å
b	-	4.59 Å	3.78 Å
c	12.99 Å	2.96 Å	9.51 Å
Density	3.95-4.03	4.3	3.8
Refractive index	1.7	2.7	2.5

To find the formation condition of rutile TiO_2 in acidic condition, we conducted experiments by adding 0.5 mL 3M $TiCl_4$ aqueous solution and (0, 0.1, 0.2, 0.5, and 1 mL) HCl solution into 20 mL deionized water in a vial and subsequent reacting them at 60 ^{o}C for 1 h under magnetic stirring. The XRD patterns of the produced TiO_2 particles in Fig. 2(a) show that the pure rutile TiO_2 phase is formed in more acidic condition (HCl = 0.5 and 1 mL in current experimental condition) and the anatase TiO_2 phase is dominantly formed in less acidic condition (HCl = 0.2, 0.1 and 0 mL in current experimental condition). This tendency is well known because 3M $TiCl_4$ aqueous solution forms stable $TiOCl_2$ and the diluted $TiOCl_2$ begins to form $[Ti(OH)_mCl_n]^{2-}$ (m+n=6), which tends to make edge sharing by condensation reaction in more acidic condition due to more existence of Cl^-, whereas it makes corner sharing in less acidic condition.[10] Fig. 2(b) is the TEM (transmission electron microscopic) image of produced TiO_2 particles in less acidic condition (HCl = 0 mL) indicating that small anatase TiO_2 nanocrystals with ~5 nm in size were synthesized. Fig. 2(c) is the SEM image of produced TiO_2 particles in more acidic condition (HCl = 1 mL) indicating the formation of relatively larger needle-shaped rutile TiO_2 primary nanoparticles with ~10 nm in size. These results imply that the rutile TiO_2 nano-shell can be directly coated on the 2D α-alumina nanoplates due to small mismatch of lattice parameter in more acidic condition, but the rough surface will be formed. Meanwhile the smooth surface can be formed in less acidic condition due to the formation of small anatase TiO_2 nanocrystals. Therefore, the coating process need to be started in more acidic condition at early reaction stage and is finished in less acidic condition at late stage in order to coat smooth TiO_2 nano-shell with small surface roughness on the 2D α-alumina nanoplates. To confirm crystal size of synthesized TiO_2 nanoparticles, we calculated the representative crystal size of anatase TiO_2 (HCl-0 mL) and rutile TiO_2 (HCl-1 mL) sample from the Scherrer equation.[11]

$$t = \frac{0.9\lambda}{B\cos\theta} \qquad (3)$$

Where t is the nanocrystal size, λ is the wavelength of the X-ray irradiation (0.154 nm), and B is the line width at half maximum (in radians). For the calculation of crystal size of anatase TiO_2 and rutile TiO_2, we used (101) peak at $2\theta = 25.3\,^{\circ}$, (110) peak at $2\theta = 27.5\,^{\circ}$, respectively. The calculated crystal size of anatase TiO_2, and rutile TiO_2 was ~ 4nm and ~ 8 nm, respectively, which was well matched with the TEM and SEM results.

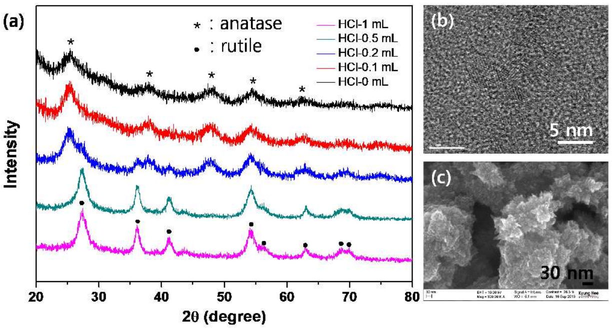

Fig. 2. (a) XRD patterns of synthesized crystalline TiO_2 particles via sol-gel method with different acidic condition. Reaction condition: 60 °C for 1h with solution mixture of 20 mL deionized water, 0.5 mL 3M $TiCl_4$ aqueous solution, and HCl aqueous solution-x mL (x = 0, 0.1, 0.2, 0.5, and 1), (b) TEM (transmission electron microscopic) image of produced TiO_2 (HCl-0 mL) in less acidic condition, and (c) SEM image of produced TiO_2 (HCl-1 mL) in more acidic condition.

To check if the rutile TiO_2 can be directly coated on the 2D α-alumina nanoplates, we coated TiO_2 nano-shell in more acidic condition by adding 0.05 g 2D α-alumina nanoplates, 1 mL HCl solution, and 0.5 mL 3M $TiCl_4$ aqueous solution into 20 mL deionized water in a vial and subsequent heating 98 °C for 2h under magnetically stirring. To check the effect of pre-treatment of 2D α-alumina nanoplates in acidic solution, we conducted again above experiment by stirring the solution mixture of 0.05 g 2D α-alumina nanoplates, 1 mL HCl solution, and 20 mL deionized water for 2h and then reacting it at 98 °C for 2h after adding 0.5 mL 3M $TiCl_4$ aqueous solution into the solution mixture. The SEM images of 2D α-alumina nanoplates coated by TiO_2 with and without HCl pre-treatment were shown in Fig. 3. This clearly indicates that the HCl pre-treatment is effective to form fully covered TiO_2 nano-shell on the surface of 2D α-alumina nanoplates because all 2D α-alumina nanoplates were coated by TiO_2 nano-shell in the HCl pre-treated sample (Fig. 3a), whereas some 2D α-alumina nanoplates were not fully covered by TiO_2 nano-shell in the sample without HCl pre-treatment (Fig. 3b and see sample image marked by arrows). The inset in Fig. 3b is magnified SEM image of the uncovered part indicating the existence of uncompleted TiO_2 coating.

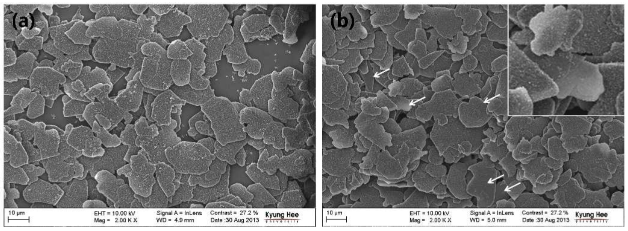

Fig. 3. SEM images of 2D α-alumina nanoplates coated by TiO_2 (a) with and (b) without HCl pre-treatment: the arrows indicate the uncovered part of 2D α-alumina nanoplates by TiO_2 and inset is a magnified image of the uncovered part.

To provide metallic gold structure colouring effect to the 2D α-alumina nanoplates, we made TiO_2 rutile and anatase mixture coating layer on the surface of 2D α-alumina if the smoother TiO_2 shell can be formed or not. For this, we pre-treated the 2D α-alumina nanoplates by stirring 0.05 g α-alumina nanoplate/20 mL deionized water/1 mL HCl solution mixture for 2h and added 0.5 mL 3M $TiCl_4$ solution into the solution at 98 °C. 0.1 mL 0.8M NaOH aqueous solution was added into the reactant solution 25 times consecutively and was reacted for 2h. Then 0.1 mL 0.8M NaOH aqueous solution was again added into the reactant solution 25 times consecutively and was reacted for 2h. The SEM image of syntheized 2D α-alumina@TiO_2 core-shell nanoplates was shown in Fig. 4(a) indicating that smoother TiO_2 shell was formed by the modified reaction than the TiO_2 shell formed in Fig. 3(a) because the rough needle-shaped rutile TiO_2 shell is likely to be formed in more acidic condition, whereas the smooth particulate anatase TiO_2 shell tends to be co-formed with rutile TiO_2 during pH adjustment by addition of NaOH.

Therefore, rutile TiO_2 might to be preferentially grown on the surface of 2D α-alumina nanoplates and the mixture of rutile and anatase TiO_2 might be co-grown on the TiO_2 layer, thereby reducing the surface roughness of TiO_2 shell. The magnified SEM image in Fig. 4(b) shows that the surface morphology is composed by needle-shaped nanoparticles and irregular smaller nanoparticles. The photograph of the dried 2D α-alumina@TiO_2 core-shell nanoplates was shown in Fig. 4(c) confirming the successful formation of TiO_2 nanoshell on 2D α-alumina nanoplates due to the appearance of gold structure colouring, whereas the pristine 2D α-alumina nanoplates exhibit silver in colour. Fig. 4(d) is the corresponding XRD patterns of the 2D α-alumina@TiO_2 core-shell nanoplates indicating that the TiO_2 shell is composed by the mixture phase of rutile and anatase TiO_2 nanocrystals as we intended to. The calculated crystal size of anatase and rutile TiO_2 in the shell from the Scherrer equation was ~8 nm and ~16 nm, respectively. The crystalline phase composition of the TiO_2 shell can be calculated from the integrated intensity of (101) peak for anatase and (110) for rutile as following equation.[12]

$$W_R = \frac{A_R}{0.886A_A + A_R} \qquad (4)$$

Where W_R is weight (mass) fraction of rutile phase, A_A is an integrated peak intensity of (101) anatase phase, and A_R is for (110) rutile phase. The calculated W_R was ~0.30 implying that the dominant crystalline phase is anatase which might help formation of smooth surface, but more fraction of anatase phase might be required to much smoother surface. The relatively rough TiO_2 shell seems to back scatter the incident light so that the intense structure colouring effect might be weakened, thereby exhibiting relatively weak lustring effect of gold in colour.

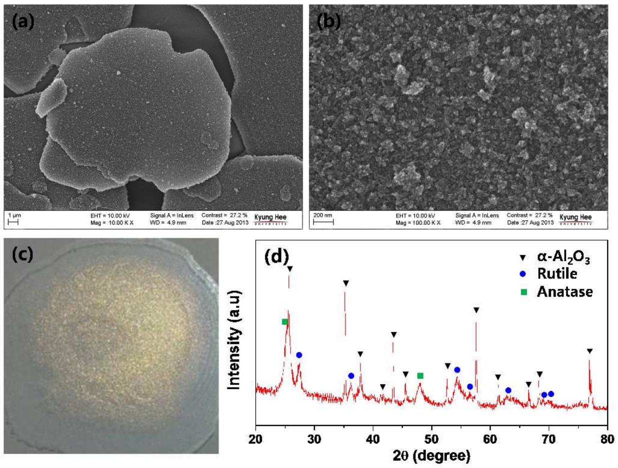

Fig. 4. (a, b) SEM images of 2D α-alumina@TiO_2 core-shell nanoplates prepared in more acidic condition: (b) magnified SEM image on top of TiO_2 shell, (c) photograph of dried 2D α-alumina@TiO_2 core-shell nanoplates on a glass substrate, and (d) their XRD patterns. (Reaction condition/procedure: 0.05 g α-alumina nanoplate/20 mL deionized water/1 mL HCl solution/0.5 mL 3M $TiCl_4$ solution/2.5 mL 0.8M NaOH aqueous solution/2.5 mL 0.8M NaOH aqueous solution)

Although the surface roughness of TiO_2 shell can be reduced by the reaction design for co-formation of rutile and anatase TiO_2 shell, the surface roughness need to be more smoothened in order to enhance lustring effect. Hence, we increased the amount of added NaOH in the reactant and additionally added Ti precursor in less acidic condition to promote the formation of anatase TiO_2 nanocrystals. For this, we stirred 0.05 g α-alumina nanoplate/20 mL deionized water/1 mL HCl solution mixture during 2h for the pre-treatment process and 0.25 mL 3M $TiCl_4$ aqueous solution was added in the reactant solution at 98 ^{o}C. 0.1 mL 0.8M NaOH aqueous solution was added into the reactant solution 37 times consecutively and was reacted for 1h. Then 0.25 mL 3M $TiCl_4$ aqueous solution was added and subsequently 0.1 mL 0.8M NaOH aqueous solution was again added into the reactant solution 37 times consecutively and was reacted for 1h. Finally, we added again 0.25 mL 3M $TiCl_4$ aqueous solution in the reaction solution and added by 37 times consecutive addition of 0.1 mL 0.8M NaOH aqueous solution. The reaction was finished after additional reaction for 2h. The SEM image of produced 2D α-alumina@TiO_2 core-shell nanoplates was shown in Fig. 5(a) and its magnified image was shown in Fig. 5(b) indicating that smoother TiO_2 shell was formed by modified reaction process. The photograph of dried 2D α-alumina@TiO_2 core-shell nanoplates in Fig. 5(c) exhibited more intense gold colour due to the reduced back scattering. Fig. 5(d) confirms that the composition of TiO_2 shell is composed by anatase and rutile phase. As we expected, the calculated W_R was ~0.22 indicating that the crystalline anatase TiO_2 is more formed than the above experimental result (see Fig. 4). Accordingly, the smoother TiO_2 nano-shell was formed by the more formation of anatase TiO_2 nanocrystals. As expected, the synthesized 2D α-alumina@TiO_2 core-shell nanoplates were not corroded by acidic (except HF solution) or basic chemicals because TiO_2 shell is very stable metal oxide.

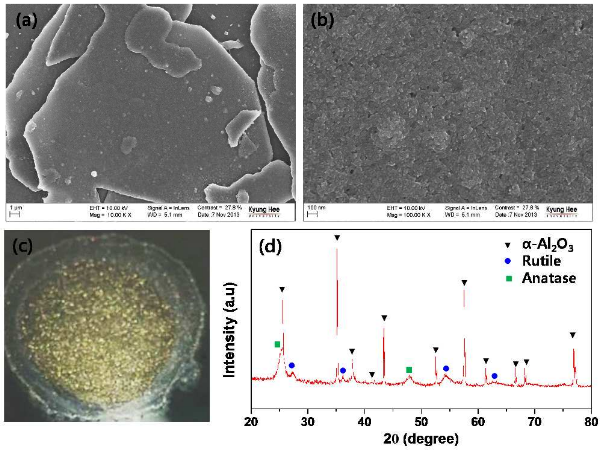

Fig. 5. (a, b) SEM images of 2D α-alumina@TiO_2 core-shell nanoplates prepared in less acidic condition: (b) magnified SEM image on top of TiO_2 shell, (c) photograph of dried 2D α-alumina@TiO_2 core-shell nanoplates on a glass substrate, and (d) their corresponding XRD patterns. (Reaction condition/procedure: 0.05 g α-alumina nanoplate/20 mL deionized water/1 mL HCl solution/0.5 mL 3M $TiCl_4$ solution/3.7 mL 0.8M NaOH aqueous solution/0.25 mL 3M $TiCl_4$ aqueous solution/3.7 mL 0.8M NaOH

aqueous solution/0.25 mL 3M $TiCl_4$ aqueous solution/3.7 mL 0.8M NaOH aqueous solution)

Conclusions

We could successfully synthesize non-corrosive 2D α-alumina@TiO_2 core-shell nanoplates showing metallic gold in colour via sol-gel solution chemistry with controlled reaction condition for the formation of anatase and rutile TiO_2 nanocrystals. When we used 0.5 mL 3M $TiCl_4$ aqueous solution/0, 0.1, 0.2, 0.5, and 1 mL HCl solution/20 mL deionized water solution mixture, the rutile phase TiO_2 was formed in more acidic condition (HCl = 0.5 and 1 mL) and the anantase phase TiO_2 was formed in less acidic condition (HCl = 0.2, 0.1 and 0 mL) because the $[Ti(OH)_mCl_n]^{2-}$ (m+n=6) intermediate complex tends to form edge sharing in more acidic condition due to more existence of Cl^- and makes corner sharing in less acidic condition. Due to small lattice mismatch between rutile TiO_2 and α-alumina nanoplates, the rutile TiO_2 could be conformably grown on the surface of α-alumina nanoplates. However, the rutile TiO_2 shell exhibited rough surface due to the formation of rough needle-shaped crystals and consequently reduced the lustring effect by the back scattering effect. The surface roughness of TiO_2 nano-shell could be further reduced by the controlled reaction of co-formation of rutile and anatase TiO_2 nanocrystals during the TiO_2 coating. The successful coating of smooth TiO_2 nano-shell on the 2D α-alumina nanoplates was associated with the fact that the rutile TiO_2 nanocrystals are preferentially coated on the 2D α-alumina nanoplates and the smaller irregular sphere-shaped anatase TiO_2 nanoparticles are co-formed on the surface of α-alumina while smoothing the surface roughness of TiO_2 nano-shell. We believe that this controlled reaction method to form smooth inorganic TiO_2 nano-shell is helpful to synthesize opalescent colour pigments, angle dependent structuring colour pigments, safety pigments, and cosmetic pearls.

Acknowledgements

This study was supported by Basic Science Research Program (No. 2014R1A5A1009799) through the National Research Foundation of Korea (NRF) funded by the Ministry of Science, ICT & Future Planning.

References

1 (a) K. S. Kim, Y. Zhao, H. Jang. S. Y. Lee, J. M. Kim, K. S. Kim, J. –H. Ahn, P. Kim, J. –Y. Choi, B. H. Hong, *Nature*, 2009, **457**, 706; (b) S. Bae, H. Kim, Y. Lee, X. Xu, J. –S. Park, Y. Zheng, J. Balakrishnan, T. Lei, H. R. kim, Y. I. Song, Y. –J. Kim, K. S. Kim, B. Özyilmaz, J. –H. Ahn, B. H. Hong, S. Ijima, *Nature Nanotechnol.*, 2010, **5**, 574; (c) J. Wu, H. A. Becerril, Z. Bao, Z. Liu, Y. Chen, P. Peumans, *Appl. Phys. Lett.*, 2008, **92**, 263302.
2 (a) H. Kim, Y. Miura, C. W. Macosko, *Chem. Mater.,* 2010, **22**, 3441; (b) Y. Su, V. G. Kravets, S. L. Wong, J. Waters, A. K. Geim, R. R. Nair, *Nature Commun.*, 2014, **5**, 4843.
3 (a) B. Radisavljevic, A. Radenovic, J. Brivio, V. Giacometti, A. Kis, *Nature Nanotechnol.*, 2011, **6**, 147; (b) S. –K. Lee, H. Y. Jang, S. Jang, E. Choi, B. H. Hong, J. Lee, S. Park, J. –H. Ahn, *Nano Lett.*, 2012, **12**, 3472; (c) C. Yan, J. H. Cho, J. –H. Ahn, *Nanoscale*, 2012, **4**, 4870.
4 (a) G. D. Moon, G. –H. Lim, J. H. Song, M. Shin, T. Yu, B. Lim, U. Jeong, *Adv. Mater.*, 2013, **25**, 2707; (b) Y. G. Seol, T. Q. Trung, O. –J. Yoon, I. –Y. Sohn, N. –E. Lee, *J. Mater. Chem.*, 2012, **22**, 23759.
5 M. Debeljak, A. Hladnik, L. Cerne, D. Gregor-Svetec, *Color Res. Appl.*, 2012, **38**, 168.
6 G. Pfaff, *Inorg. Mater.*, 2003, **39**, 123.
7 (a) V. Štengl, J. Šubrt, S. Bakardjieva, A. Kalendova, P. Kalenda, *Dyes and Pigments*, 2003, **58**, 239; (b) P. M. T. Cavalcante, M. Dondi, G. Guarini, F. M. Barros, A. B. Luz, *Dyes and Pigments*, 2007, **74**, 1; (c) M. Ren, H. Yin, A. Wang, T. Jiang, Y. Wada, *Mater. Chem. Phys.*, 2007, **103**, 230; (d) Q. Gao, X. Wu, Y. Fan, X. Zhou, *Dyes and Pigments*, 2012, **95**, 534.
8 (a) S. Teaney, G. Pfaff, K. Nitta, *Eur. Coat. J.*, 1999, **4**, 90; (b) S. Sharrock, N. Schuel, *Eur. Coat. J.*, 2000, **1/2**, 20.
9 E. Hecht, Optics, Pearson Education, Inc., Addison Wesley, 4th Ed. Chap. 4 & 9.
10 H. Cheng, J. Ma, Z. Zhao, L. Qi, *Chem. Mater.,* 1995, **7**, 663.
11 B. D. Cullity, S. R. Stock, Elements of X-ray diffraction, Pearson, 2001.
12 (a) J. Yu, Y. Su, B. Cheng, *Adv. Funct. Mater.*, 2007, **17**, 1984; (b) T. H. Han, H. –S. Moon, J. O. Hwang, S. I. Seok, S. H. Im, S. O. Kim, *Nanotechnol.*, 2010, **21**, 185601.